CHEMISTRY
A EUROPEAN JOURNAL

DOI: 10.1002/chem.201001477

3rd EuCheMS Chemistry Congress

# Functional Hybrid Materials with Polymer Nanoparticles as Templates

Anitha Ethirajan[a, b] and Katharina Landfester*[a]

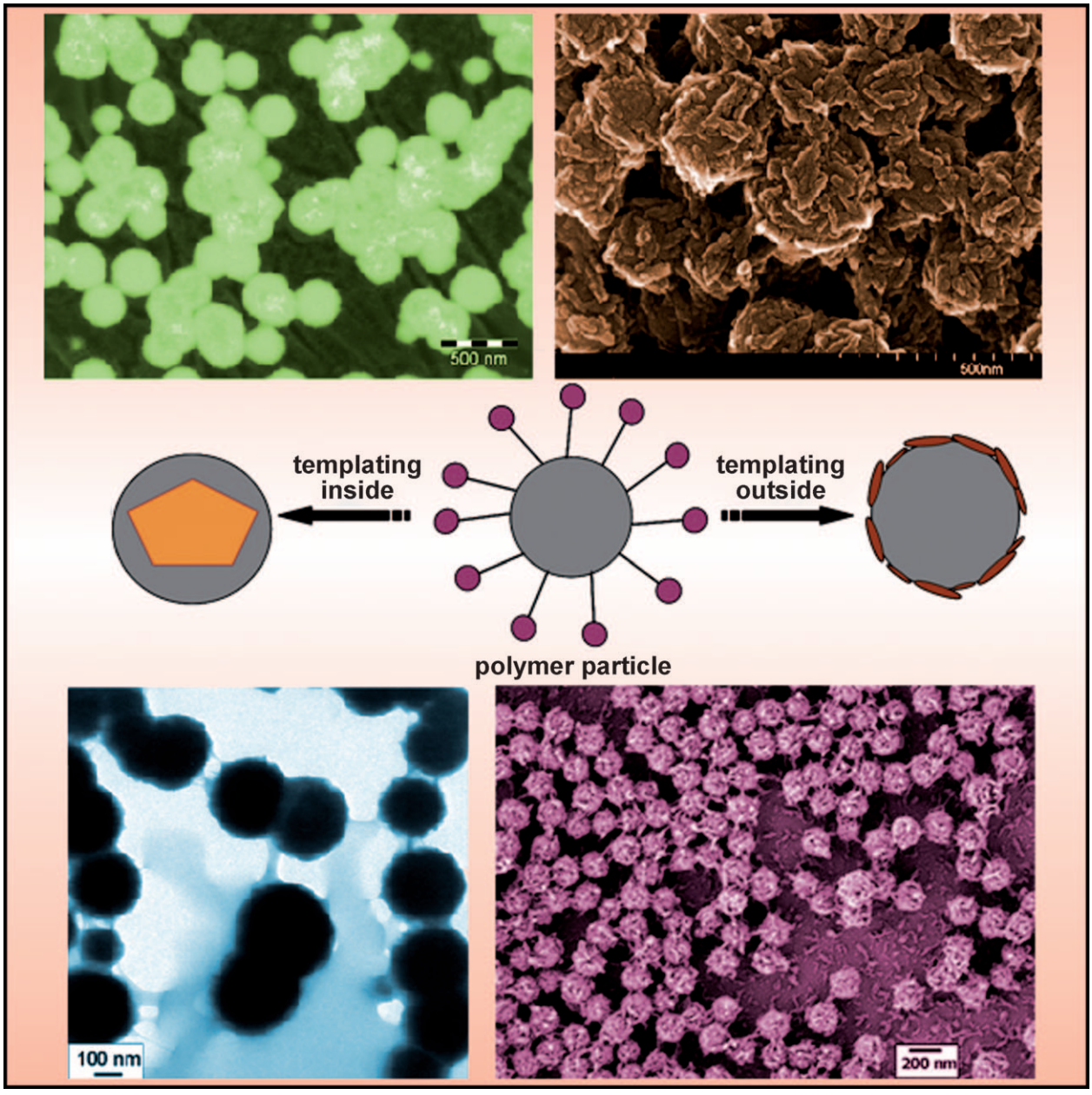

**Abstract:** The use of polymeric nanoparticles as templates for producing inorganic materials is an intriguing approach as it offers the feasibility of synthesizing hybrid organic–inorganic functional materials for a broad spectrum of applications ranging from optoelectronics to biomedicine. The concept of using polymer nanoparticles as templates to produce hybrid materials has several advantages. On the one hand, the entire geometry of the nanoparticle can be used as a confined nano-environment to let the inorganic material grow inside the particle. On the other hand, the high surface area of nanoparticle can be exploited to let the inorganic material grow on the outside surface of the particles. One such application is presented here, in which polymer nanoparticles were used as biomimetic template to produce composite nanoparticles made of the bone mineral hydroxyapatite (HAP). The synthesized hybrid particle has a great potential to be used as regenerative filler or as scaffold for nucleation and growth of new bone material. In addition to be applied as coatings on implants, these nanoparticles also offer the feasibility of being injected directly into the damaged part or administered intravenously with functionalization. Within this overview, we will mainly focus on different polymer nanoparticles obtained by the miniemulsion technique and the different possibilities for them to be used as templates for the biomimetic mineralization of calcium phosphate in the aqueous phase.

**Keywords:** biomimetic synthesis · miniemulsions · nanoparticles · polymers · template synthesis

## Introduction

The urge for developing new nanoscaled materials is paralleled by attempts to develop new techniques to produce them. Nature has ever been an inspiration for mankind and serving as a treasure-trove of concepts to design and develop new materials and novel methods. Some of the creations in nature have fascinated mankind owing to their functional values paired with aesthetic values. One such creation are the biominerals, which are abundantly found in nature with fascinating shapes and colors and have been optimized by the evolutionary process to perform unique functions. The complex yet intriguing architectures over several hierarchy levels in combination with superior functional properties and how nature builds them are often far from imagination of mankind. However, these are the principle reasons that inspire researchers from various fields of interests. The field of "biomineralization" has been the focus of interest for several decades to unravel the mysteries entangling these fascinating objects. To learn the underlying concepts of the natural processes and applying these concepts to produce advanced functional materials as well as mimicking the process itself to synthesize some of these biological architectures are the driving forces for the rapidly developing field called "biomimetic or bio-inspired materials syntheses".[1,2] This review will mainly focus on the synthesis of an organic–inorganic hybrid material, namely polymer–hydroxyapatite (bone mineral and thermodynamically stable form of calcium phosphate) based on a biomimetic synthetic strategy.

[a] Dr. A. Ethirajan, Prof. Dr. K. Landfester
Max Planck Institute for Polymer Research
Ackermannweg 10, 55128 Mainz (Germany)
Fax: (+49) 6131-379-370
E-mail: landfester@mpip-mainz.mpg.de

[b] Dr. A. Ethirajan
Current Address: Institute for Materials Research (IMO)
Hasselt University, Wetenschapspark 1, 3590 Diepenbeek (Belgium)

## Templates for Organic–Inorganic Hybrid Functional Materials

Although hybrid materials can also be produced by the incorporation of preformed inorganic materials into a polymeric matrix by blending and grinding,[3] they are often limited in scope with respect to the organic–inorganic interface integrity, spatial dimensions, and practical applicability. Several synthetic strategies aimed to implement the lessons learnt from nature into the in vitro syntheses has led to the use of interesting approaches, such as employing templates for mineralization, soluble additives as crystal growth modifiers, and so forth. The feasibility to control shape, size, crystal structure, and orientation, and the organization of inorganic colloids in polymeric matrices has led to biomimetic approaches being intensively explored to produce interesting hybrid materials. Some examples of conceptual approaches for the synthesis of hybrid nanoparticles (here, containing calcium phosphate) are based on employing organic additives or templates, such as surfactants,[4–6] liposomes,[7,8] block copolymers,[9,10] self-associated nanogels,[11] supramolecular hydrogels,[12] emulsions, and microemulsions.[13–15] Besides the possibilities to play with several control parameters, such approaches involving the matrix mediation and the molecular templating for mineralization have shed light on the interfacial chemistry between the organic and inorganic components as well as the mechanisms of crystallization in association with the co-reactants.[16,17] Therefore, the use of templates for mineralization is a very fruitful strategy as it not only allows the synthesis of hybrid materials with interesting properties, but also sheds some light for a better understanding of the underlying biomineralization concepts. For these aforementioned reasons, new templates based on different material composition and design archietectures, for example, supramolecular assem-

  

blies, self-assembled monolayers (SAMs), and polymeric nanoparticles, have constantly been explored.

## Polymer Nanoparticles as Templates

The concept of using polymer nanoparticles as templates to produce hybrid materials has several advantages: on the one hand, the entire geometry of the nanoparticle can be used as a confined nano-environment to grow the inorganic material inside the particle and on the other hand, the high surface area of nanoparticle can be exploited to grow the inorganic material on the outer surface of the particles. As a prerequisite for templating on both the inside and outside of nanoparticles, the functional groups are required to be present in the respective places of the polymer nanoparticle. This can be achieved by using different types of polymers or combinations for forming polymer nanoparticles.

Although the concept of using polymeric nanoparticles as templates for synthesizing inorganic materials[18,19] is very much enticing and promising, it is still in its infancy with respect to several terms and conditions. To start with, it demands a technique that can produce stable nanoparticles with well-defined properties and is versatile enough to tailor the template nanoparticles with respect to the desired applications, for instance tuning of the nanoparticle size and flexibility by the choice of materials used. One such technique which facilitates the synthesis of nanoparticles in a simple straight forward route, taking into account the above mentioned criteria along with other advantages, is the miniemulsion technique.[20,21]

Within this overview, we will mainly focus on different polymer nanoparticles obtained by the miniemulsion technique and the different possibilities for such nanoparticles being employed as templates for the biomimetic mineralization of calcium phosphate (CaP) in the aqueous phase.

## Synthetic Possibilities by the Use of Miniemulsions

In spite of the existence of several heterophase processes that allow the formation of polymer nanoparticles and nanocapsules, the miniemulsion technique holds a fortified position in the synthesis of nanoparticles and hybrid nanoparticles.[22,23]

The general concept of miniemulsions can be viewed as a process in which a heterophase system is subjected to high shear forces in order to generate small, homogeneous, and stable droplets of precursor materials in a continuous phase. The nanoparticle production using the miniemulsion process is shown in Figure 1. The size of droplets is tunable from

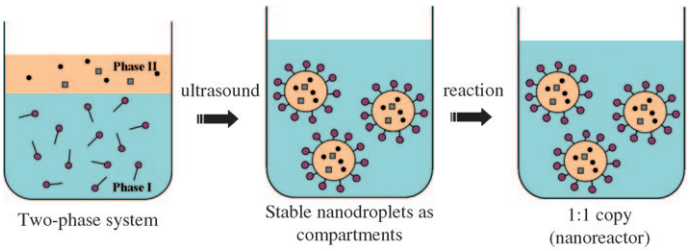


Figure 1. Scheme of the miniemulsion process.

30–500 nm and is mainly dependent on the type and the amount of the emulsifier used in the particular system. The miniemulsion working principle is based on the concept of a nanoreactor in which each of the droplets can be treated as an individual entity or a nanoreactor for performing different reactions. The precursor material could be inorganic or organic materials (monomers) or a mixture of both. The ver-

*Anitha Ethirajan studied engineering for her B.Sc. and specialized in the field of polymers. She received her degree (first rank holder; honoured with gold medal) in 2002 from the University of Madras, Chennai (India). Then, she studied for her M.Sc. in advanced materials in 2004 from Institute of Solid State Physics, Ulm University (Germany); she received a DAAD scholarship during this period. She pursued her doctoral studies (2004–2008) on the topic: "Polymeric nanoparticles synthesized through miniemulsion process as templates for biomimetic mineralization" under the guidance of Prof. Dr. Katharina Landfester, Institute of Macromolecular Chemistry and Organic Materials, Ulm University (Germany). Afterwards, she worked at the Max-Planck Institute for Polymer Research, Mainz (Germany) for the period 2008–2010 as a post-doc researcher in the research group Physical Chemistry of Polymers (Prof. Dr. K. Landfester). Recently, she joined the Biosensor group (Prof. Dr. P. Wagner) in the Materials Physics part of the Institute for Materials Research (IMO), Hasselt University as a post-doc researcher.*

*Katharina Landfester studied chemistry at the technical university of Darmstadt (Germany). For her diploma thesis, she was at the Ecole d'Application des Hautes Polymères in Strasbourg (France) under the guidance of Prof. M. Lambla. In 1995, she received her Ph.D. in physical chemistry from the Johannes Gutenberg University of Mainz (Germany) after working with Prof. H. W. Spiess at the Max Planck Institute for Polymer Research on the synthesis and characterization of core-shell latexes by transmission electron microscopy and solid-state NMR spectroscopy. After spending another year as a group leader at the institute, she moved for a post-doctoral stay at the Lehigh University (USA) in the group of Prof. M. El-Aasser, where she first came in contact with the miniemulsion technique. She returned to Germany in 1998 joining the group of Prof. M. Antonietti at the Max Planck Institute of Colloids and Interfaces in Golm. There, she led the miniemulsion group working on new possibilities in the synthesis of complex nanoparticles. In 2002, she got her habilitation in physical chemistry at the University of Potsdam. In 2003, she accepted a Chair of Macromolecular Chemistry at the University of Ulm. She became a director at the Max Planck Institute for Polymer Research in 2008.*

satility of the technique can be evidenced from the possibilities offered by this technique to perform reactions that are pragmatically limited by other heterophase polymerizations, such as suspension, emulsion, and dispersion polymerization, to produce polymer nanoparticles.[24]

The flexibility in particle design and formation through the use of miniemulsions can be achieved by adopting appropriate start-up procedures based on the "ingredients" used as well as by combining different synthetic approaches in one system. As this versatile technique allows the fabrication of polymeric nanoparticles by the polymerization of respective monomers, as well as by using preformed polymers, polymer nanoparticles from biopolymers and synthetic polymers can be produced. In this review, the use of the preformed gelatin (a biopolymer) and aliphatic polyester (synthetic biodegradable polymers) polymers and the synthetic biocompatible poly(styrene-*co*-acrylic acid) and poly(styrene-*co*-phosphonic acid) copolymers for the nanoparticle formulation using miniemulsion methods will be described. Subsequently, the use of such polymer nanoparticles formulated by using different synthetic approaches, for example, employing different templating strategies (see Figure 2) for the calcium phosphate mineralization in the aqueous phase, will be discussed in detail.

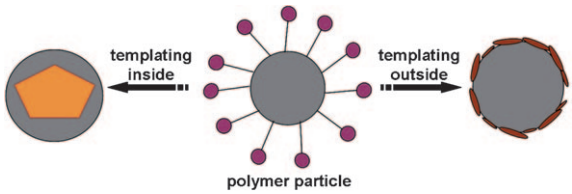


Figure 2. Scheme illustrating different templating strategies using (surfactant-stabilized) polymer nanoparticles.

## Templating Inside: Crystallization Inside the Nanoreactor

For using the entire volume of the nanoparticle as a template, it is essential that the functional groups that can bind the ions are distributed randomly in the polymer chain that comprises the polymer nanoparticle. In this section, two different preformed polymers, gelatin—a processed biopolymer—and aliphatic polyesters—synthetic biodegradable polymers—formulated in to nanoparticles by using different approaches by the miniemulsion technique will be described. Subsequently, the use of these nanoparticles employed as nanoreactors for the biomimetic mineralization of CaP will be discussed in detail.

**Processed biopolymer-based nanoparticles**: Gelatin, an indispensable raw material in both the pharmaceutical and food industry, owing to its chemical and physical nature, has been a promising candidate for template-based syntheses.[25,26] The intrinsic biocompatibility, ability to interact with hydroxyapatite (HAP) mineral surfaces, and its low cost makes it an interesting candidate for the biomimetic mineralization of CaP for use in tissue-engineering applications. Gelatin is basically a proteinaceous polyampholytic gel obtained by the partial hydrolysis (acidic or basic) of collagen. Depending on the process used, gelatin is produced as type-A or type-B gelatin. While the acidic treatment yields type-A gelatin with an isoelectric point (pI) around 9 and a broad molecular-weight profile, the alkaline hydrolysis yields type-B gelatin with a pI around 5.[27,28] The abundant functional groups offer the advantage of incorporating more functionalities and introducing modifications through chemical derivatization.

Gelatin as a matrix for biomimetic mineralization has been studied under various conditions.[25,26,29,30] Although the encapsulation of preformed HAP in a gelatin matrix and coprecipitation or precipitation of HAP in gelatin solution or gels are interesting, the composite scaffolds in these cases are either lacking an organic–inorganic interface integrity, owing to direct blending in the matrix, or they are very large and thus pragmatically limited. In a different approach, as gelatin is soluble in water, composite microspheres of apatite–gelatin, produced by using the water-in-oil technique, were reported and the size of the resulting composites ranged from few to several micrometers (10–100 μm).[31,32] Although mineralization using gelatin matrix in the aqueous phase in a heterophase system is challenging, cross-linked gelatin nanoparticles could circumvent the solubility issue. Such microgel particles would ideally serve as a spatially restricted nanoenvironment and molecular template for inorganic mineralization, as the size of the pore for the diffusion of the ions and the ratio of organic–inorganic components can be tailored.

The synthesis of stable gelatin nanoparticles is highly interesting and advantageous, as these microgel reactors allow the potential application for the release of a variety of different components. On the one hand, the incorporated drug molecules can be released by the volume transition induced by temperature as an external stimulus. On the other hand, the presence of amino and carboxyl functional groups, which in turn offer the possibility of functionalization with fluorescent and bone markers, make gelatin nanoparticles an ideal candidate for biomedical applications.

As gelatin is a preformed hydrophilic polymer, it is not possible to form nanoparticles directly in aqueous solution. In this case the formulation process should be carried out in a way such that the polymer chains have to be chemically cross-linked. This allows the retention of the nanoparticulate structure in the aqueous phase, even at elevated temperature or at low or high pH values.

Several techniques have been used to synthesize gelatin nanoparticles from gelatin and gelatin derivatives. Well-established techniques are the desolvation,[33–37] the coacervation,[38–40] and water-in-oil emulsion techniques.[41–43] The flexibility offered by these techniques in tailoring the properties of the nanoparticles is limited. With increasing gelatin concentration and by using a gelatin with a broad molecular-weight distribution, it is not possible to effectively and

  

uniformly achieve high gelatin content within the particles. In the desolvation technique, the final particle yield constitutes about only 70–75% of the original amount of gelatin used. About 40% of free gelatin chains were still present irrespective of the amount of cross-linker used.[34] The coacervation and desolvation techniques are both based on phase separation during the preparation step; the cross-linking step is performed after phase separation, in which the nanoparticles are already formed and gelatin chains are no longer in the dissolved state. Due to diffusion problems of the cross-linker molecules into the interior of the nanoparticles, cross-linking only occurs at the surface, and chains in the interior are not cross-linked resulting in inhomogeneous cross-linking of the nanoparticles with free polymer chains. Among the water-in-oil emulsion techniques, the emulsifier-free water-in-oil approach leads to relatively large particles with an average size range of 840 nm.[43] The use of the water-in-oil microemulsion approach in order to obtain smaller particles, however, demands a large excess of surfactant; the ratio of gelatin to surfactant can be as high as 1:1600.[42] The degree of cross-linking with increasing gelatin concentration and scalability to industrial production are often limited.

To overcome the aforementioned problems in producing uniformly glutardialdehyde-cross-linked gelatin nanoparticles with a high gelatin concentration, a convenient synthetic route based on the concept of nanoreactors (individual nanosized homogeneous entities) using the miniemulsion technique has been used.[21] The scheme illustrating the synthesis of gelatin nanoparticles is presented in Figure 3.

The miniemulsion technique is a straight forward approach, since it does not rely on the phase separation and offers the flexibility of easily varying the gelatin content and the degree of cross-linking by using small amounts of surfactant.[44] For the preparation of homogeneously cross-linked nanoparticles, a gelatin solution is miniemulsified at elevated temperature above the helix–coil transition temperature in a hydrophobic continuous phase, resulting in a stable inverse miniemulsion. By adding a second inverse miniemulsion, consisting of aqueous droplets with the cross-linking agent glutaraldehyde, in the same continuous phase as before, the cross-linking reaction can be performed by a fission and fusion process between the different droplet species. The technique allows one to use different types of gelatin without purification or fractionation in addition to varying the amount of the gelatin in the droplet and the degree of cross-linking over a wide range. However, it is of interest to use a minimum of cross-linking agent such that all chains are cross-linked and no free chains are left within the particles. It is demonstrated that, independent of the molecular weight distribution of the gelatin used, stable nanoparticles can be produced with a small amount of surfactant. After the synthesis, the organic solvent can be removed and the particles can be transferred to an aqueous continuous phase. The stability of the dispersion, particle size, morphology, and the efficiency of cross-linking by analyzing the uncross-linked free chains have been studied in detail.[44] As the gelatin can undergo the volume transition induced by temperature as stimuli, the swelling behavior of the gelatin particles can be seen, when these nanoparticles in water are subjected to a thermal cycle changing the temperature between 20–45 °C: particles sizes of about 230 nm at 20 °C and 250 nm at 45 °C were determined by dynamic light scattering (DLS). The larger size at elevated temperatures is due to the lack of physical cross-linking and therefore a more pronounced swelling.

These cross-linked gelatin nanoparticles, prepared in inverse miniemulsions and transferred to the water phase, act as defined individual nanoreactors; they serve as an ideal molecular organic template providing the spatial confinement for CaP mineralization in the aqueous phase to form hybrid particles.[45]

The microgel particles were loaded as shown in Figure 4 with calcium ions by complexation with the carboxyl ions present in the gelatin chain followed by the addition of phosphate ions for the formation of hydroxyapatite at a constant pH of 10. The gelatin particles were sequentially loaded with ions in order to form composite hybrid HAP/gelatin nanoparticles and allow the possibility to study the influence of confinement on the growth and transformation mechanism of the calcium phosphate phase, which are controlled on the molecular level through ion complexing with the carboxyl or amino ions. The combination of selected area electron diffraction (SAED) and XRD were used to determine the inorganic phase unambiguously, while the transmission electron microscopy

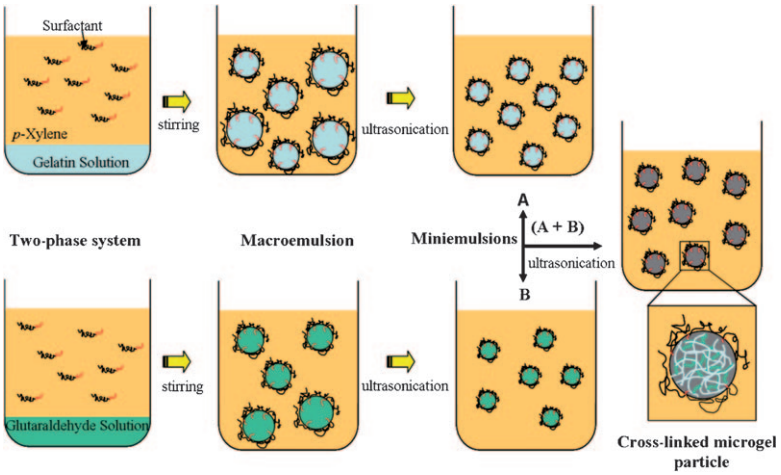


Figure 3. Synthesis of gelatin nanoparticles using the inverse miniemulsion process.

  

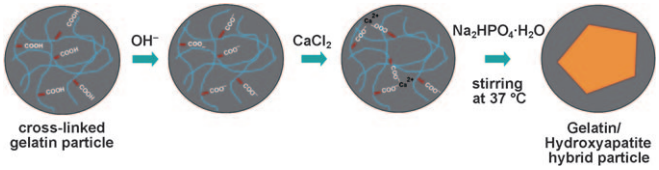


Figure 4. Schematic representation of using cross-linked gelatin nanoparticles as templates for the growth of hydroxyapatite to form hybrid particles.

(TEM) images were used to confirm the crystal growth inside the particle.[45] Figure 5 shows the hybrid particles prepared by using gelatin nanoparticles.

As gelatin nanoparticles themselves have a very weak contrast in the TEM, the presence of the inorganic phase in the matrix gives a strong contrast in the TEM micrographs. As with the dark-field imaging mode, more information about the inorganic phase was obtained from the same sample. It was found that different types of particles (see Figure 5c) co-exist at the same time: 1) particles that possess a uniform contrast without crystalline reflections within the particle, 2) particles that display strong crystalline reflections, and 3) particles in which there is a non-uniform contrast but no indications for crystalline reflections, rather reflecting only the orientation of the crystals with respect to the incident electron beam not matching any Bragg condition. The SAED on these particle types shed light to the different crystal phases present in the hybrid particle.

The particles of type 1 without any crystalline region inside the particle exhibited a wide and diffuse pattern in the SAED revealing that they are amorphous (see Figure 6). As very exhaustive studies[46–50] have already been performed on the transformation of metastable amorphous calcium phosphate (ACP) to the stable HAP phase, a detailed characterization of the crystalline region containing particles was carried out. TEM images and SAED from the hybrid particle (see Figure 7) revealed that inside the nanoreactor the HAP grows as a single crystal; particles of type 2 showed diffraction spots with a six-fold symmetry and the calculated *d*-spacing proved that the formed material was HAP.

It was confirmed that the crystal phase present inside the particle was not an electron-beam-induced artifact, as the particles that showed the amorphous-like electron diffraction pattern were not affected on exposure to a highly converged electron beam for a considerable time period. Since no crystalline features were induced in the particle, it confirms that the crystals inside the particles were formed by solution mediated phase transformation.

As the aim was to obtain HAP, it was necessary to know if the transformation of the phases happens at the physiological temperature in a reasonable timescale or not. This was studied by performing XRD on samples that were stirred at 37 °C for different periods of time (see Figure 8).

The sample that showed different types of particles co-existing at the same time in the TEM (see Figure 5c) gave an XRD pattern with the superposition of amorphous and crystalline regions, confirming the TEM results on that sample. It was also found that by increasing stirring period, the amorphous contribution decreased and the characteristic Bragg peaks of HAP developed at the expense of the amor-

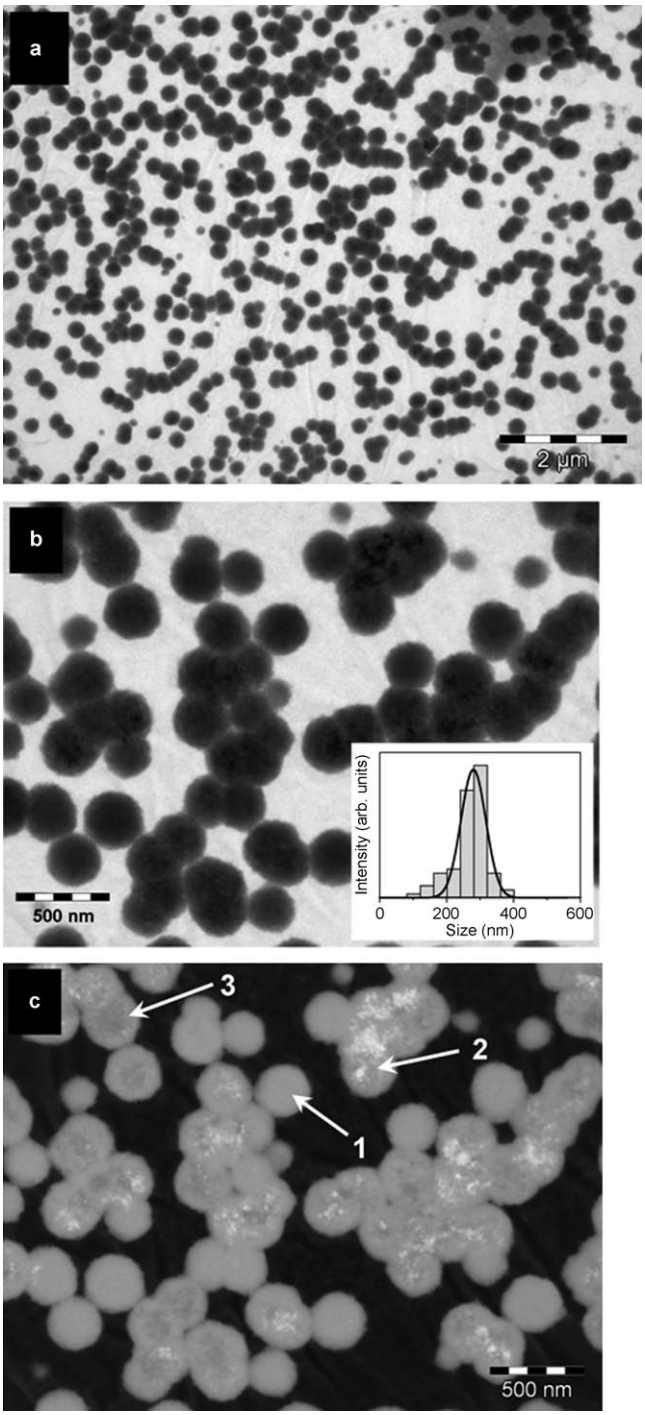


Figure 5. Hybrid gelatin nanoparticles: a) bright-field image over a large region; b) bright-field image of a characteristic region with the particle size distribution in inset; c) dark-field image of the area shown in b) to illustrate the presence of crystals inside the particle taken with the (300) reflection; the arrows indicate the presence of different kinds of particles (for details see text).[45]

  

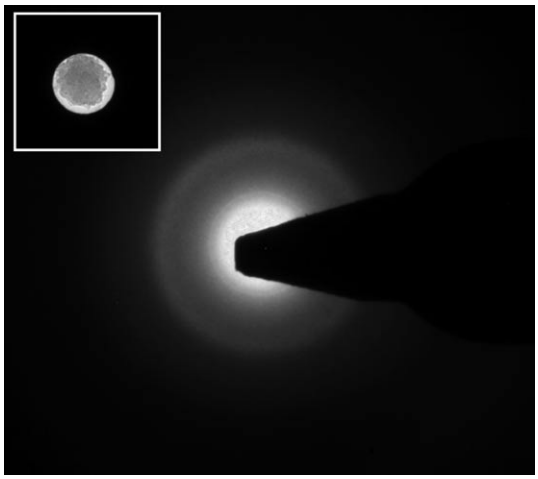

Figure 6. Typical amorphous electron-diffraction pattern of the gelatin/HAP particle of type 1 shown in inset.[45]

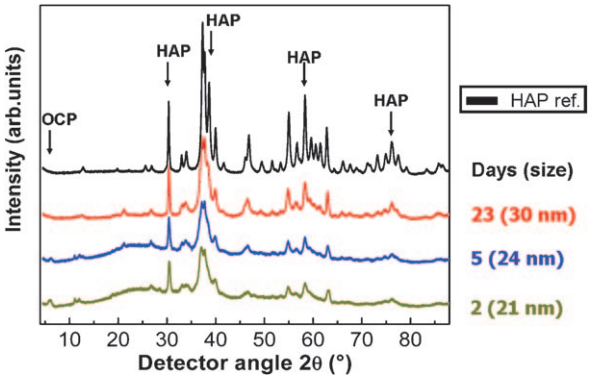


Figure 8. XRD pattern of HAP reference ($Ca_{10}(PO_4)_6(OH)_2$) and salt-loaded gelatin particles after different time periods of stirring. The arrows labeled HAP indicate the increased intensities and the development of characteristic peaks of HAP at the marked positions, while the arrow labeled as OCP indicates the tiny trace of the corresponding phase present.

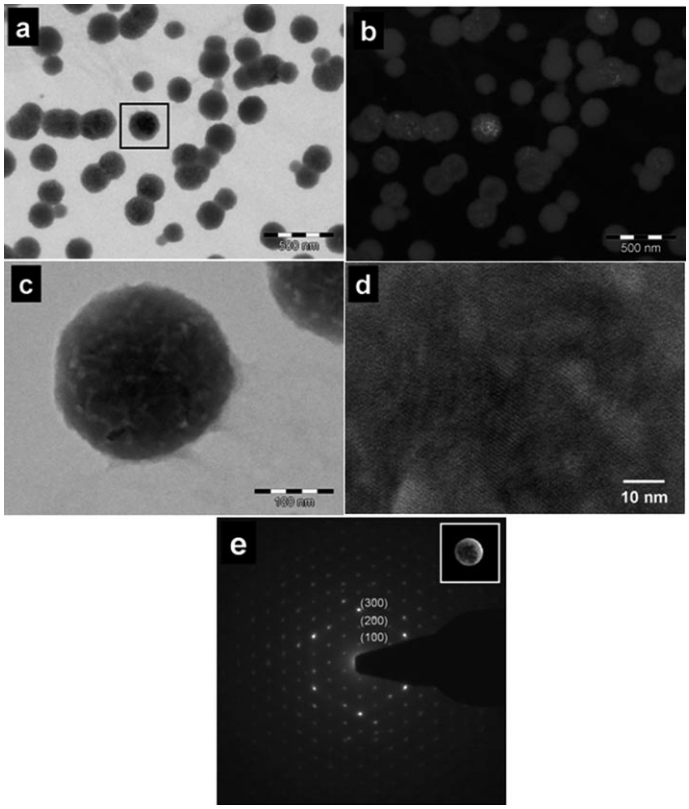


Figure 7. a) Bright-field image of a typical region in the TEM grid with the particle of type 2 to be characterized shown in the rectangle; b) corresponding dark-field image of the same region shown in a); c) enhanced image of the hybrid particle shown in the rectangle in a); d) high-resolution image showing the internal structure of the same particle shown in c), in which the single-crystalline nature without domains could be seen; e) SAED pattern from the complete single particle shown in inset and the respective reflections of HAP are indicated.[45]

phous fraction. The characteristic Bragg peaks, which sharpened with time, reflected the increase in size of the crystallites. It is worth noting that all the samples were maintained at 37 °C during these studies. This is very important because, all these transformations happened at the physiological temperature on a reasonable timescale without additional heat treatment. This allows the use of the ACP-containing hybrid particles for bone repair applications, transforming into the thermodynamically stable HAP in the body on a reasonable time scale.

In addition to this finding, there was a small fraction of octacalcium phosphate (OCP) that was present in the initial stages of transformation from ACP to HAP. This was an indication that the OCP phase is an intermediate phase formed in the earlier stages during the transformation from ACP to HAP; it was not possible to detect with the TEM as it is a local probing technique. So, in this case, we can say that the mineralization inside the particles follows Ostwald's rule of stages, in which an initially formed amorphous CaP phase transforms into single crystalline hydroxyapatite via an octacalcium phosphate intermediate without any calcination step.

A significant advantage of this technique is that the hybrid particles could be produced with different HAP contents in physiological conditions. As these gelatin-based hybrid colloids can aggregate and physically cross-link together at $T < 37$ °C, depending upon the application and optimizing them with respect to mechanical properties and porosity can lead to the fabrication of biomimetic high-performance ceramics, bioimplants, and bone or teeth cements. This biomimetic approach offers the advantage of preserving the hierarchical organization of organic–inorganic components and can be extended to develop new hybrid materials for a wide range of technological applications.

**Synthetic biodegradable polymer-based nanoparticles**: The synthetic biopolymers have advantages over natural polymers as they could be synthesized with a high degree of reproducibility with defined physicochemical properties. The most investigated biodegradable synthetic polymers for tissue engineering are based on saturated polyesters like

  

poly(L-lactic acid) (PLLA), poly(glycolic acid) (PGA), poly(ε-caprolactone) (PCL), and poly(D,L-lactide-*co*-glycolide) (PLGA). As these polyesters possess biodegradability, biocompatibility, and low toxicity in vivo, they have found use in the biomedical field as long-circulating carriers for the controlled release of drugs.[51–53] The chemical properties of these polymers allows hydrolytic degradation through ester hydrolysis.[54] The degradation occurs by uptake of water followed by the hydrolysis of the ester bonds. Several factors play a role in the degradation kinetics of these polymers, such as the chemical composition, the molar mass, environmental conditions, the crystallinity, the hydrophobicity, and so forth.[55–63]

The incorporation of hydroyapatite (HAP) in these resorbable polyester matrixes can be obtained, for example, by blending preformed HAP in the polymeric matrix,[64,65] encapsulating HAP within microspheres,[66] and by fabrication of PLGA/HAP composite scaffolds using the gas-forming and particulate-leaching methods for bone-tissue engineering.[67] In a different approach, surface grafting of degradable polymer onto the nano-HAP surface by using radio-frequency plasma polymerization in order to improve the adhesion within PLGA matrix for better mechanical properties has been performed.[68] Several other interesting methods for fabricating porous composite scaffolds by using biodegradable polymers have also been reported.[3]

Biomimetic approaches have been postulated to mineralize biodegradable polymeric scaffolds.[69] The hydrolytic degradation properties of these polymers could be exploited for the mineralization of scaffolds. The saponification induced by strong alkali (NaOH) leads to the generation of carboxylate groups, which can be subsequently used to bind calcium. It has been shown that the NaOH hydrolysis of poly(ε-caprolactone), poly(lactide-*co*-glycolide), and poly(L-lactic acid) leads to an increased mineralization of polymer surfaces compared to identical non-hydrolyzed polymers.[70–72]

Previously, Jabbarzadeh et al.[73] studied the mineral formation on the surface of poly(lactide-*co*-glycolide)-sintered microsphere scaffolds. The microspheres were of several hundred micrometers in size. Hence, using nanoparticles synthesized from these polymers for such a template approach could be thought of as an excellent biomimetic strategy to produce composite particles for tissue-engineering applications owing to the pragmatic applicability.

The synthesis of biodegradable polyester particles in a sub-micron range by a combination of the solvent evaporation and the miniemulsion technique was recently reported.[74] The polymer nanoparticles were prepared by emulsifying the organic phase, containing the preformed polymer (dispersed phase), in an aqueous phase, containing a water soluble surfactant. The subsequent application of high shear led to the formation of monodisperse droplets in a size range of 150–300 nm. At this point the polymer is expected to be homogeneously distributed within all of the droplets and after the removal of the organic solvent by evaporation, the polymer precipitates to form solid nanoparticles. The scheme showing the synthesis using preformed polymers and electron micrographs of the obtained particles produced are presented in Figure 9. The optimized synthesis of these particles taking into account several parameters like the

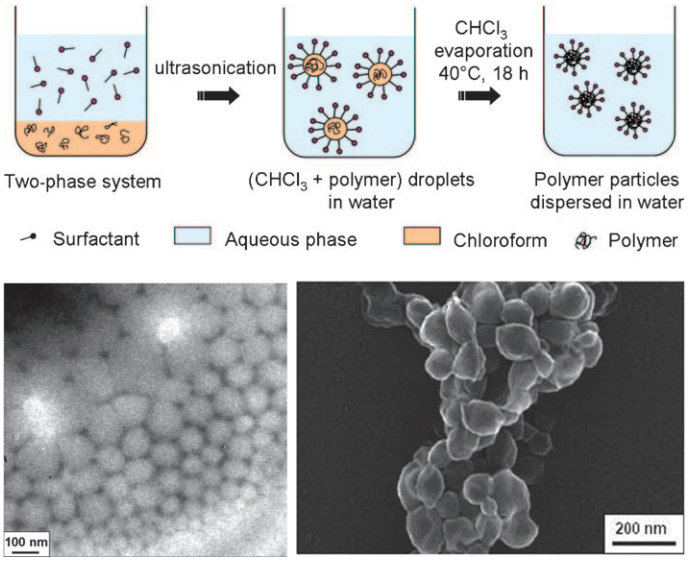


Figure 9. Top: Nanoparticle formulation by employing preformed polymers with a combination of emulsion/solvent evaporation methods and the miniemulsion technique. Bottom: TEM (left) and SEM (right) micrographs of PLLA particles.

choice and amount of the surfactant, the amount of polymer and the molecular weight, as well as varying oil-to-water ratios with respect to the particle size and particle size distribution have been already reported.[74]

Interestingly, the nanoparticles synthesized by means of the miniemulsion technique have the added advantage as possible use in template applications. As mentioned before, although the primary mechanism of degradation of these aliphatic polyesters occur through hydrolysis of backbone ester groups, it is necessary to consider the degradation occurring during the ultrasonication step throughout the miniemulsion formation.[75] It was found that PLLA or PCL nanoparticles, produced by the miniemulsion method, showed a reduction in the molecular weight of the polymer depending on the nature of the polymer-type used.[74] The principal reason for such a loss in molecular weight was ascribed to the thermal degradation of the polymer induced by the high shear during ultrasonication step. Thus, the degradation caused by random hydrolytic cleavage of ester bonds due to the alkali treatment (providing increased density of anionic functional group) as well as the intrinsic degradation that was present in the nanoparticles prior to any treatment (due to the ultrasonication step) were taken for granted and these particles were exploited as templates for the calcium phosphate (CaP) mineralization.[76]

The hydrolysis treatment was performed at 37 °C for a prolonged time by the addition of alkaline NaOH. The increase in the amount of carboxylic and hydroxyl groups, due

  

to the scission of polyester chains, serves to bind the calcium ions to the polymeric template particle, promoting heterogeneous mineral growth. The hydrolyzed particles were loaded with calcium ions followed by phosphate ions for CaP mineralization at a constant pH of 10. The composite particles presented in Figure 10 in comparison with the unloaded

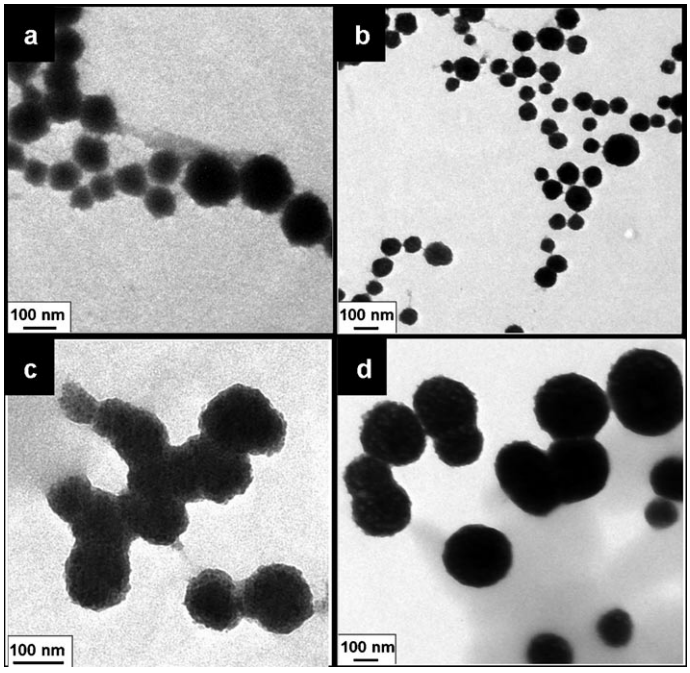


Figure 10. TEM micrographs of CaP composite particles prepared by using a) high-molecular-weight PLLA, b) low-molecular-weight PLLA, c) low-molecular-weight PCL, and d) high-molecular-weight PCL particles.

pure polymer nanoparticles (TEM micrograph in Figure 9, bottom left) show a relatively strong and homogeneous contrast, indicating that the inorganic phase is well distributed within the particle. The inorganic phase present in the particles was characterized by using different imaging modes, energy dispersive X-ray (EDX) spectroscopy, and SAED by using an electron microscope. The chemical composition of the composite particles studied using EDX spectroscopy proved the presence of calcium, phosphorous, and oxygen. The presence of several tiny crystallites in the particle was seen in the magnified dark-field image (see Figure 11). The bright spots arising from the amorphous background studied by means of SAED revealed that the tiny crystallites are indeed HAP crystals.

In a different approach, preformed hydroxyapatite can also be embedded in the biodegradable polymeric matrices to form composite nanoparticle.[76] The hybrid particles could be applied for bone-repair applications, as coatings on implants, or as a building block for the scaffold fabrication that might be able to nucleate and grow new bone material. Although, such encapsulation within the polymeric matrix has already been reported in the form of microspheres,[66] encapsulation in the form of nanoparticles possess added ad-

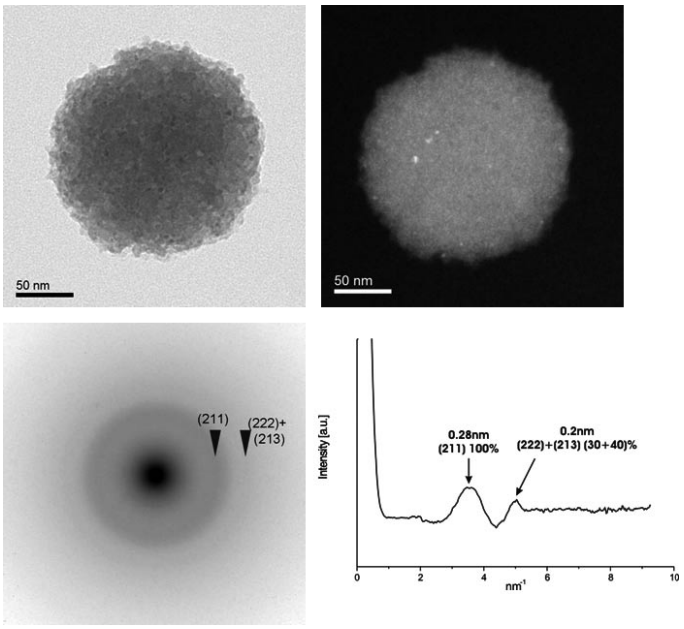


Figure 11. Bright- (left) and dark-field (right) TEM micrographs of CaP composite particles prepared by using low-molecular-weight PLLA (top row). Electron diffraction (ED) pattern with arrows indicating the diffraction rings (bottom left) and the corresponding profile calculated from the ED (bottom right).

vantages as they offer several possibilities for final applications owing to their large surface area and homogeneity. For the formulation of such hybrid particles, a reliable technique that allows a high homogeneity, solid content, and entrapment efficiency is decisive. All these criteria are accomplished by the miniemulsion process, for which materials like pigments,[77,78] fluorescent marker,[74,79] and magnetite[80] have already been reported to be efficiently encapsulated. The hybrid particles can be formed by encapsulating the preformed nano-hydroxyapatite into the biodegradable poly(lactic acid) matrix by slightly optimizing the miniemulsion technique.[74,76] As the nanoapatite crystals are relatively hydrophilic and the polymer hydrophobic, the encapsulation in aqueous phase is difficult. The polymer–inorganic interface compatibility plays a crucial role in the encapsulation efficiency. To ease the encapsulation difficulties, the nanoapatites were coated with block copolymeric surfactant in chloroform to hydrophobize them and to separate the crystals from each other. The hydrophobized nanoapatites were then added to the dispersed phase comprising of PLLA and chloroform for encapsulation by using the emulsion/solvent evaporation in combination with the miniemulsion technique. The morphology of the hybrid particles and the encapsulation efficiency can be evidenced from the TEM and SEM images in Figure 12.

The incorporation of the apatite nuclei into the polymer particle, as well the extended hydrolysis to improve the calcium ion binding of the polymer chain, can accelerate and enhance the CaP mineralization in these polymer particles. Also, another interesting and important aspect of using

  

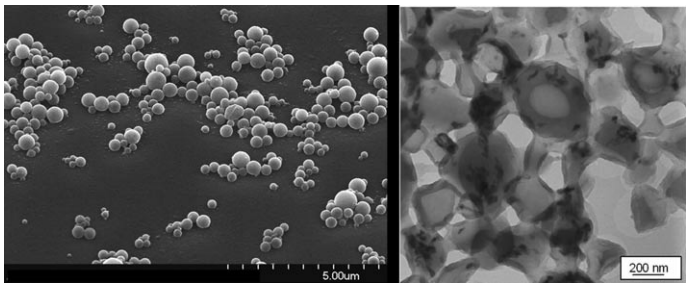


Figure 12. SEM (left) and TEM (right) micrographs of nanoapatite encapsulated PLLA particles.

these nanoparticles synthesized by the miniemulsion technique is the possibility of encapsulating biomolecules and drugs; the release of growth factors and antibiotics could enhance the bone growth in the treatment of bone defects and support wound healing.

## Templating Outside: Crystallization Outside on the Functionalized Surface

Despite the complexity involved in nature's biomineralization processes, the basic premise of surface functionalization to induce mineral deposition can be mimicked in the laboratory. The role of glycoproteins (osteonectin, phosphoproteins) and γ-carboxyglutamic acid (Gla) proteins (osteocalcin) has been observed and discussed in close association with the mineralization front.[81–84] Although the whole mineralization mechanism of bone and teeth is not completely understood, due to interplay of several factors, it is assumed that the anionic groups present in these proteins act as chelators of ionic species (Ca ions) present in the surrounding media, thus stimulating crystal nucleation. The use of phosphonate and carboxyl groups as functional groups is therefore very interesting to study the influence of different surface functional groups in the biomimetic synthesis of CaP.

In this context, the surface of the polymer particle can be functionalized with the appropriate functional groups in order to attract the ions to the surface to form hybrid particles, with crystals forming only on the surface of the polymer particle. Although, there are several possible functional groups that can be used for the mineralization of CaP, the synthetic possibilities are very much limited in order to obtain to hybrid particles with inorganic materials only on the outer surface of the nanoparticles.

**Surface functionalized polymer nanoparticles**: Surface-functionalized nanoparticles can be exploited as templates for the growth of hydroxyapatite crystals on the polymeric nanoparticle surface. Tamai and Yasuda[85] have reported the synthesis of HAP-coated polymer particles by employing $Pd^0$-immobilized poly(styrene-*co*-acrylic acid) copolymer particles synthesized by emulsifier-free emulsion polymerization. Later, the formation of HAP nanocrystals on the surface of β-diketone-functionalized polymeric nanoparticles, by employing styrene and acetoacetoxyethyl methacrylate (AAEM), obtained by emulsifier-free emulsion polymerization was reported.[86] The carboxylated polystyrene latex particles have also been used for the preparation of other inorganic materials like $Ag/Ag_2O$.[87] However, in these above-mentioned studies the amount of functional groups was always fixed and the amount of inorganic material precipitated was controlled by controlling either the reaction parameters[85,87] or the amount of added respective salts.[86] In previous studies of self-assembled monolayers (SAMs) with several anionic functional groups on Ti wafers, it was shown that $-COOH$ and $-PO_4H_2$ functional groups can nucleate HAP.[88] Thus, the use of carboxylated and phosphonated functionalized polymer particles templates seems to be a practical way to synthesize hybrid colloids with highly crystalline HAP.

The synthesis of functionalized polystyrene particles by miniemulsion polymerization has been well-studied and documented.[79] The miniemulsion technique allows the synthesis of various surface-functionalized polystyrene particles with different amounts of charged groups bound to the surface by varying the amount of functional co-monomers and surfactant types.[79,89] The focus was on carboxylated and phosphonated funtionalized polymeric nanoparticles produced by the miniemulsion copolymerization of respective monomers (see Figure 13) and their use as template for CaP mineralization on the surface of the template particle (see Figure 14).

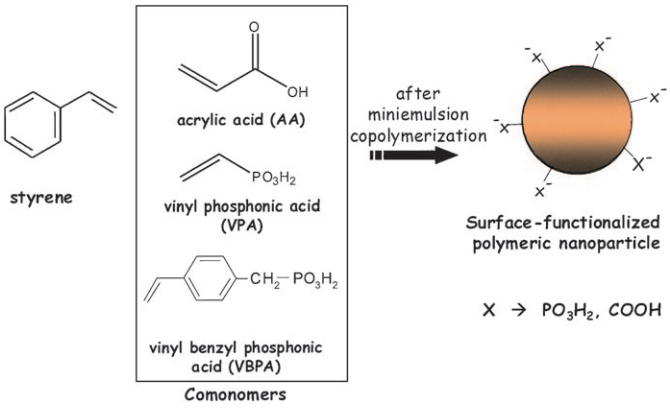


Figure 13. Surface-functionalized particles that can be prepared using direct miniemulsion (oil-in-water) employing different comonomers.

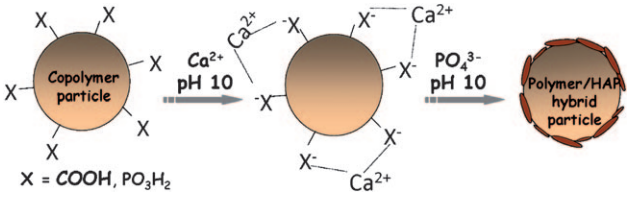


Figure 14. Scheme of surface-functionalized nanoparticles as template for biomimetic mineralization of hydroxyapatite (HAP).

  

**Carboxylated polymer nanoparticles**: Surface-functionalized particles with covalently bound carboxyl groups prepared by using both ionic and nonionic surfactants were used as templates to perform crystallization on the surface of the particles. This approach of crystallization outside the particle is in contrast to the previous approach,[45] in which the crystallization was performed inside gelatin nanoparticles that served as a confined reaction environment. The influence of the type of surfactant with respect to particle size, density of functional surface groups, and HAP formation on carboxyl-functionalized latex particles were studied in detail.[90]

A clear tendency of an increasing number of charge groups with an increasing acrylic acid (AA) content was seen in case of both ionic and nonionic surfactant types. When using nonionic surfactants for producing latexes, an increased instability was observed with increasing co-monomer AA content. This was attributed to the bridging of the latex particles by the polymeric chains, the increased viscosity, and the reduction in the efficiency of steric stabilization caused by a specific interaction between ethylene oxide chains of the Lutensol AT50 molecules and carboxyl groups.[91–95] Despite such a limitation, the nonionic surfactant was efficient in preparing carboxyl-functionalized particles with a high surface charge density with low amounts of the comonomer AA.

Also, it was observed that, for the same acrylic acid content, the average surface charge density of carboxyl groups for particles prepared with the nonionic surfactant Lutensol AT50 was higher than for particles prepared with the ionic surfactant sodium dodecylsulfate (SDS). This was attributed mainly to the competition of SDS with AA at the particle–water interface, owing to their ionic nature. As the aim of preparing these functionalized particles was to use them as templates for HAP growth, the ionic surfactant stabilized particles were dialyzed extensively to remove SDS and exchanged with the non-ionic surfactant Lutensol AT50 for an additional steric stabilization against electrolyte addition.

Hybrid nanoparticles were formed by performing crystallization outside on the surface of the polymer nanoparticles prepared with varying amount of surface functional groups.[90] The HAP formation on the surface of the particle was carried out by the addition of calcium ions followed by a dropwise addition of phosphate ions, corresponding to the stoichiometric $Ca^{2+}$:$PO_4^{3-}$ ratio for hydroxyapatite [$Ca_{10}(PO_4)_6(OH)_2$] formation, at a constant pH of 10. For all types of particles, the loading with ions could be performed without impairing the colloidal stability. The carboxyl-functionalized particles prepared using different amounts of comonomer after mineralization can be seen in the SEM images for different surfactant types in Figures 15 (ionic surfactant) and 16 (nonionic surfactant).

It was found that, for a fixed concentration of $Ca^{2+}$ and $PO_4^{3-}$ ions added, the amount of crystals formed on the surface of the particles increased with increasing AA amount. The crystals formed were proven to be hydroxyapatite by XRD. The absence of HAP on the particle surfaces for latexes prepared with 0 wt% AA for both ionic and nonionic surfactant types confirms that the amount of HAP formed depends only on the amount of carboxyl groups present on the surface. It was found that HAP formation was pronounced for particles prepared with nonionic surfactant, which is in agreement with the high amount of −COOH groups as compared to the latexes prepared with SDS as anionic surfactant. However, it was also found that, in addition to high carboxyl functionalization on the surface of the particles, it is absolutely necessary to have an optimum surfactant concentration for particles prepared with nonionic surfactant to obtain high HAP nanocrystal formation.

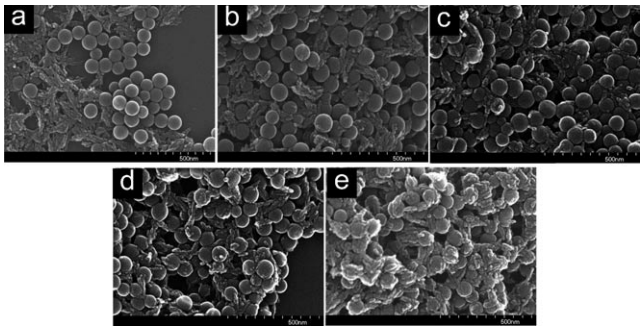


Figure 15. HRSEM images illustrating the HAP formation with particles prepared using different amounts of acrylic acid as co-monomer employing an ionic surfactant. a) 0 wt% AA; b) 1 wt% AA; c) 3 wt% AA; d) 5 wt% AA; and e) 10 wt% AA.[90]

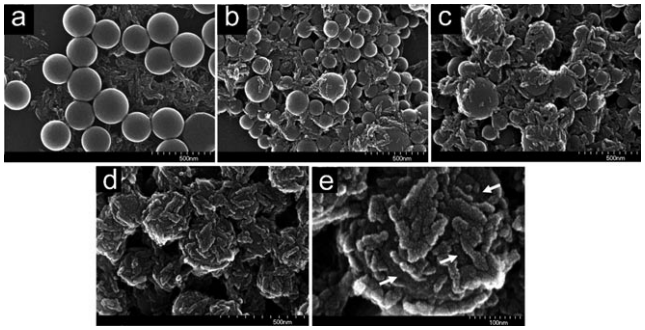


Figure 16. HRSEM images illustrating the HAP formation with particles prepared using different amounts of acrylic acid as co-monomer employing a non-ionic surfactant. a) 0 wt% AA; b) 1 wt% AA; c) 2 wt% AA; and d) 3 wt% AA. e) Particle in d) shown in higher magnification to see the surface coverage. The arrows indicating the underlying polymeric core nanoparticle show that the complete coverage of the surface with the crystals is not yet achieved.[90]

**Phosphonated polymer particles in comparison to carboxylated particles**: The phosphonate groups are very promising as functional groups in binding Ca ions as they are diprotic in nature as compared to the carboxylic groups. In addition, the phosphonate groups show a strong tendency to adhere to the metal oxide substrates through acid–base interactions,[96–99] thereby serving as an efficient anchor group when used on metal oxide based bioimplant surfaces. The significance of pyrophosphate and organic bisphosphonates in vitro mineralization were explored as early as 1969.[100] Also,

  

the effective binding to HAP crystals has led to the wide spread use of a variety of organic bisphosphonates as physiological regulators for bone resorption in medicine.[101] Thus, the phosphonate-functionalized particles are ideal for tissue engineering applications as the surface phosphonate groups can nucleate HAP as well as anchor to the implant surfaces.

The synthesis of phosphonic acid functionalized particles by using the miniemulsion technique were recently reported.[102] As the miniemulsion technique allows for convenient tailoring of the surface-functionalized-particle properties by varying the type and amount of the co-monomers, phosphonate-functionalized polymer particles were prepared by using different co-monomers with varying hydrophilicity.[102,103] The solubility of the functional-group-containing co-monomer in the dispersed as well as continuous phase is very crucial in a copolymerization reaction, as it will determine the net incorporation of the co-monomer in the polymer chain and the amount of functional groups that will be available on the particle surface. Two different co-monomers namely vinyl phosphonic acid (VPA), a highly water soluble monomer and vinylbenzyl phosphonic acid (VBPA), an oil-soluble monomer were used for the copolymerization with styrene to form phosphonate-functionalized polymer particles. It was found that particles synthesized with the more hydrophobic VBPA monomer contain a higher amount of surface functional groups relative to those obtained in the presence of VPA. The particles were then used as templates to perform CaP crystallization on the surface of the particles. As CaP nucleation and growth is very much dependent on the reaction parameters like pH and temperature, the influence of such parameters were studied in detail for these particles and were compared with carboxyl-functionalized particles.[104] As the use of nonionic surfactants—in addition to their stability against electrolyte addition—was efficient in preparing carboxyl functionalized particles with a high surface charge density and thus high coverage of particles with HAP crystals, all the phosphonate and carboxyl functionalized particles for comparative study were prepared using nonionic surfactant.[90]

The influence of different surface functional groups on the mineralization was studied by loading the particles at a constant pH of 10 with calcium ions followed by phosphate ions in stoichiometric ratio of 5:3 to form HAP.[104] The surface-functionalized particle used for this study were prepared by using different co-monomers at respective concentrations that gave the highest amount of surface functional groups (3 wt% AA, 10 wt% VPA, and 5 wt% VBPA). The SEM images (see Figure 17) proved that, irrespective of the functional groups and in the absence of functional group, the formed crystals had needlelike crystal morphology under the given reaction conditions. It was clearly shown that there was no crystal formation on the particle surfaces for particles prepared without a co-monomer. It was also demonstrated that, independent of the type of functional co-monomer used, the amount of hydroxyapatite crystals formed on the particle surface depends only on the number

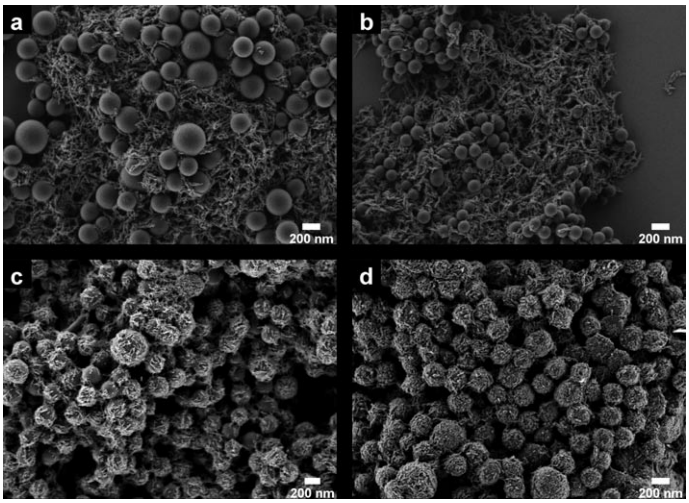


Figure 17. SEM images of different surface-functionalized polystyrene particles loaded with hydroxyapatite at pH 10: a) without co-monmer (0 groups per $nm^2$), b) with VPA as comonomer (0.4 phosphonate groups per $nm^2$), c) with AA as co-monomer (2.6 carboxyl groups per $nm^2$), and d) with VBPA as comonomer (3.3 phosphonate groups per $nm^2$).

of negative charges on the particle surface. The mineral phase formed on all the particle surfaces was proven to be hydroxyapatite by XRD.

It was found that, changing the pH for the mineralization resulted in completely different crystal morphologies.[104] The surface-functionalized particles that were mineralized at different pH are shown in Figure 18. At pH 10 HAP was formed with a needlelike morphology and at pH 7 HAP crystallized in the form of platelets. On the other hand, at pH 5 an amorphous shell of calcium phosphate built around the polymeric template was found. In contrast to carboxyl-functionalized particles, in which the crystal density decreased with decreasing pH, in the case of VBPA as functional co/monomer, an almost complete surface coverage with crystals was found under different loading conditions. The complexation of calcium ions to the particle surface, analyzed by titration studies in the first step of the mineralization, showed that this effect arises due to different amounts of negatively charged surface groups, depending on the degree of deprotonation of the functional groups. Studies on the kinetics of mineralization showed that the morphology of the HAP crystals on the surface of the polymer particles can be effectively controlled by changing the crystallization rate and thus the driving force for HAP growth through a thoughtful choice of pH. This might be of great importance for its potential application as a bone filler or implant coating, as the performance of a biomaterial could be strongly influenced by the hybrid particle morphology. The colloidal stability after the hybrid particle formation could be restored by either addition of ionic surfactant like sodium dodecylsulfate (SDS) or nonionic polymer like polyvinylpyrrolidone (PVP) to the particle dispersion.

The adhesion forces measured between the particles adhered on a silicon wafer sputtered with 20 nm $TiO_2$ and a ti-

  

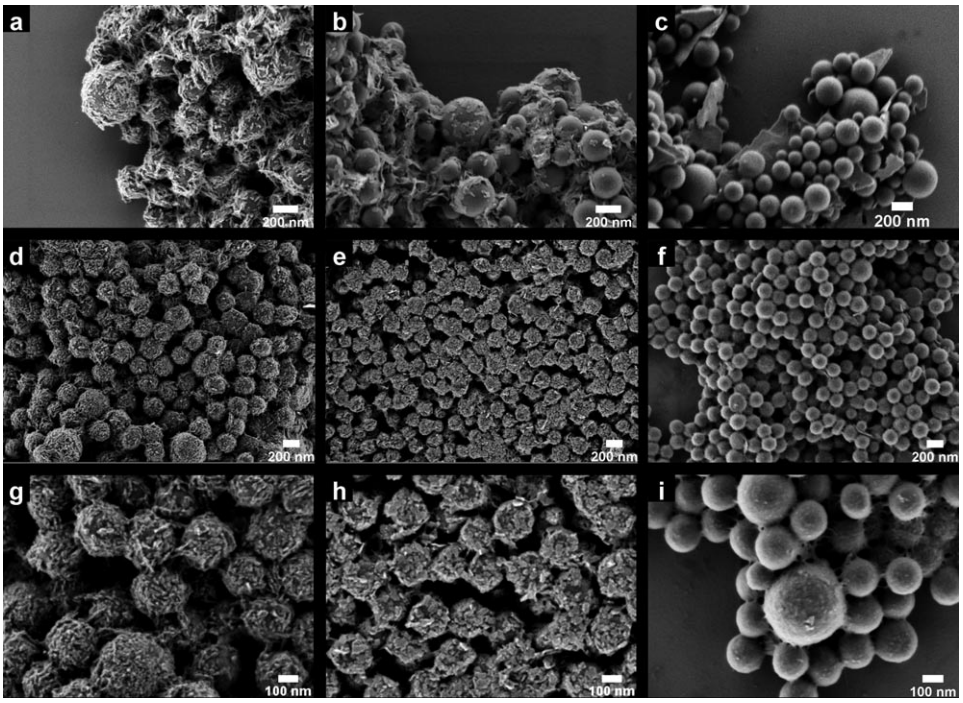


Figure 18. SEM images of carboxyl functionalized particles (a–c) and phosphonate functionalized particles in low magnification (d–f) and high magnification (g–i), loaded at pH 10 (first column: a,d,g), pH 7 (second column: b,e,h) and pH 5 (third column: c,f,i).

## Summary and Outlook

The versatile miniemulsion technique has been exploited successfully to prepare different types of polymeric template nanoparticles that were used for the crystallization of hydroxyapatite. It has been demonstrated that the miniemulsion technique is a very simple and straight forward approach to produce homogeneous stable nanoparticles with tailored properties from biopolymers, as well as synthetic biocompatible and biodegradable polymers. It was shown that both the volume as well as the surface of the polymer particles can be used as templates for the biomimetic mineralization. The mineralization was carried out in an environment friendly manner, without using extreme conditions of temperature or pressure, as all the phase transformations involving amorphous calcium phosphate to crystalline hydroxyapatite occurred under physiological conditions (37 °C). These hydroxyapatite/polymer hybrid nanoparticles have great potential to be used as fillers or as a scaffold for nucleation and growth of new bone material. They offer the feasibility of being injected directly into the damaged part, in addition to being applied as coatings on implants. Also such particles for bone-repair applications open new doors for realizing the potential of using biodegradable polymeric nanoparticles as carriers of drugs and growth factors to better treat bone defects and promote wound healing. In general, such a benign approach applying the simple concept of using polymeric nanoparticles as templates and mimicking the biomineralization process opens new vistas in the template-assisted mineralization to fabricate various functional hybrid materials with well-defined properties.

tanium dioxide AFM tip was $13.4 \pm 0.9$ nN for pure polystyrene particles and $63.9 \pm 4.3$ nN for polystyrene particles functionalized with phosphonate anchor groups.[103] As the strong adhesion forces between the phosphonated polystyrene particles and the metal oxide surfaces was proven by AFM studies, they can be used as a promising candidates for the functionalization of implant surfaces. Also, as the phosphonate groups were successfully employed for the nucleation of calcium phosphate in solution, a monolayer of phosphonate-functionalized particles formed on titania surface could serve as an effective nucleation site with its high density of surface phosphonate groups. As a proof of principle experiment, it was shown that such particle-functionalized surfaces could be used as a potential system for bone mineralization.[103] The functionalized particle layer was sequentially loaded with calcium and phosphate ions with the stoichiometric ratio of 5:3 to form hydroxyapatite at the physiological temperature of 37 °C. The mineral formed on the surface of the particle can be visualized in the SEM image in Figure 19. It was found that neither the salt addition nor the stirring at 37 °C were able to disrupt the particle layer, indicating negligible influence on the particle adhesion. All the particles were densely covered by the crystals proving the homogeneity of the crystal formation on the particle similar to the observations with the phosphonate functionalized particles dispersed in solution and mineralized.[104] The mineral phase formed on the particle surface was proven to be hydroxyapatite by XRD, in an analogous mineralization experiment in which crystallization was performed with the VBPA functionalized particles in solution.

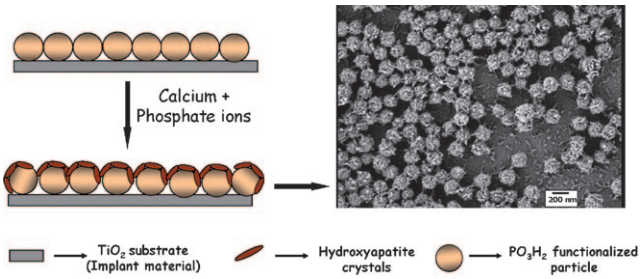


Figure 19. Crystal formation on the surface of polystyrene-polyVBPA particles adhered on a titania surface.

  

[1] S. Mann, *Biomineralization: Principles and Concepts in Bioinorganic Materials Chemistry*, Oxford University Press, Oxford **2001**.
[2] A.-W. Xu, M. Yurong, H. Cölfen, *J. Mater. Chem.* **2007**, *17*, 415–449.
[3] K. Rezwan, Q. Z. Chen, J. J. Blaker, A. R. Boccaccini, *Biomaterials* **2006**, *27*, 3413–3431.
[4] C. E. Fowler, M. Li, S. Mann, H. C. Margolis, *J. Mater. Chem.* **2005**, *15*, 3317–3325.
[5] S. Sarda, M. Heughebaert, A. Lebugle, *Chem. Mater.* **1999**, *11*, 2722–2727.
[6] T. Welzel, W. Meyer-Zaika, M. Epple, *Chem. Commun.* **2004**, 1204–1205.
[7] H. T. Schmidt, B. L. Gray, P. A. Wingert, A. E. Ostafin, *Chem. Mater.* **2004**, *16*, 4942–4947.
[8] H. T. Schmidt, A. E. Ostafin, *Adv. Mater.* **2002**, *14*, 532–535.
[9] M. Antonietti, M. Breulmann, C. G. Göltner, H. Cölfen, K. K. W. Wong, D. Walsh, S. Mann, *Chem. Eur. J.* **1998**, *4*, 2493–2500.
[10] Y. Kakizawa, K. Miyata, S. Furukawa, K. Kataoka, *Adv. Mater.* **2004**, *16*, 699–702.
[11] A. Sugawara, S. Yamane, K. Akiyoshi, *Macromol. Rapid Commun.* **2006**, *27*, 441–446.
[12] Z. A. C. Schnepp, R. Gonzalez-McQuire, S. Mann, *Adv. Mater.* **2006**, *18*, 1869–1872.
[13] G. K. Lim, J. Wang, S. C. Ng, L. M. Gan, *Langmuir* **1999**, *15*, 7472–7477.
[14] K. K. Perkin, J. L. Turner, K. L. Wooley, S. Mann, *Nano Lett.* **2005**, *5*, 1457–1461.
[15] D. Walsh, J. D. Hopwood, S. Mann, *Science* **1994**, *264*, 1576–1578.
[16] M. Breulmann, H. Cölfen, H.-P. Hentze, M. Antonietti, D. Walsh, S. Mann, *Adv. Mater.* **1998**, *10*, 237–241.
[17] S.-H. Yu, H. Cölfen, *J. Mater. Chem.* **2004**, *14*, 2124–2147.
[18] J. Hain, A. Pich, H.-J. P. Adler, *Macromol. Symp.* **2007**, *254*, 128–135.
[19] J. G. Zhang, S. Q. Xu, E. Kumacheva, *J. Am. Chem. Soc.* **2004**, *126*, 7908–7914.
[20] K. Landfester, *Adv. Mater.* **2001**, *13*, 765–768.
[21] K. Landfester, *Annu. Rev. Mater. Res.* **2006**, *36*, 231–279.
[22] K. Landfester, *Angew. Chem.* **2009**, *121*, 4556–4576; *Angew. Chem. Int. Ed.* **2009**, *48*, 4488–4507.
[23] K. Landfester, A. Musyanovych, V. Mailänder, *J. Polym. Sci. Part A: Polym. Chem.* **2010**, *48*, 493–515.
[24] K. Landfester, *Macromol. Rapid Commun.* **2001**, *22*, 896–936.
[25] R. Kniep, P. Simon, *Top. Curr. Chem.* **2007**, *270*, 73–125.
[26] H. Tlatlik, P. Simon, A. Kawska, D. Zahn, R. Kniep, *Angew. Chem.* **2006**, *118*, 1939–1944; *Angew. Chem. Int. Ed.* **2006**, *45*, 1905–1910.
[27] K. B. Djagny, Z. Wang, S. Xu, *Crit. Rev. Food Sci. Nutr.* **2001**, *41*, 481–492.
[28] R. Schrieber, H. Garies, in *Gelatine Handbook: Theory and Industrial Practice*, Wiley-VCH, Weinheim **2007**.
[29] A. Bigi, E. Boanini, S. Panzavolta, N. Roveri, *Biomacromolecules* **2000**, *1*, 752–756.
[30] S. Busch, U. Schwarz, R. Kniep, *Adv. Funct. Mater.* **2003**, *13*, 189–198.
[31] H.-W. Kim, B.-H. Yoon, H.-E. Kim, *J. Mater. Sci. - Mater. Med.* **2005**, *16*, 1105–1109.
[32] S. Teng, L. Chen, Y. Guo, J. Shi, *J. Inorg. Biochem.* **2007**, *101*, 686–691.
[33] S. Azarmi, Y. Huang, H. Chen, S. McQuarrie, D. Abrams, W. Roa, W. H. Finlay, G. G. Miller, R. Löbenberg, *J. Pharm. Pharm. Sci.* **2006**, *9*, 124–132.
[34] S. Balthasar, K. Michaelis, N. Dinauer, H. V. Briesen, J. Kreuter, K. Langer, *Biomaterials* **2005**, *26*, 2723–2732.
[35] C. J. Coester, K. Langer, H. Von Briesen, J. Kreuter, *J. Microencapsulation* **2000**, *17*, 187–193.
[36] C. A. Farrugia, M. J. Groves, *J. Pharm. Pharmacol.* **1999**, *51*, 643–649.
[37] J. J. Marty, R. C. Oppenheim, P. Speiser, *Pharm. Acta Helv.* **1978**, *53*, 17–23.
[38] E. Leo, M. A. Vandelli, R. Cameroni, F. Forni, *Int. J. Pharm.* **1997**, *155*, 75–82.
[39] K. W. Leong, H. Q. Mao, V. L. Truong-Le, K. Roy, S. M. Walsh, J. T. August, *J. Controlled Release* **1998**, *53*, 183–193.
[40] R. C. Oppenheim, N. F. Stewart, *Drug Dev. Ind. Pharm.* **1979**, *5*, 563–571.
[41] M. G. Cascone, L. Lazzeri, C. Carmignani, Z. Zhu, *J. Mater. Sci. Mater. Med.* **2002**, *13*, 523–526.
[42] A. K. Gupta, M. Gupta, S. J. Yarwood, A. S. G. Curtis, *J. Controlled Release* **2004**, *95*, 197–207.
[43] J. K. Li, N. Wang, X. S. Wu, *J. Microencapsulation* **1998**, *15*, 163–172.
[44] A. Ethirajan, K. Schoeller, A. Musyanovych, U. Ziener, K. Landfester, *Biomacromolecules* **2008**, *9*, 2383–2389.
[45] A. Ethirajan, U. Ziener, A. Chuvilin, U. Kaiser, H. Cölfen, K. Landfester, *Adv. Funct. Mater.* **2008**, *18*, 2221–2227.
[46] N. C. Blumenthal, A. S. Posner, *Calcif. Tissue Res.* **1973**, *13*, 235–243.
[47] A. L. Boskey, A. S. Posner, *J. Phys. Chem.* **1973**, *77*, 2313–2317.
[48] E. D. Eanes, I. H. Gillessen, A. S. Posner, *Nature* **1965**, *208*, 365–367.
[49] A. S. Posner, F. Betts, *Acc. Chem. Res.* **1975**, *8*, 273–281.
[50] J. D. Termine, E. D. Eanes, *Calcif. Tissue Res.* **1972**, *10*, 171–197.
[51] I. Bala, S. Hariharan, M. N. V. R. Kumar, *Crit. Rev. Ther. Drug Carrier Syst.* **2004**, *21*, 387–422.
[52] O. Benny, M. Duvshani-Eshet, T. Cargioli, L. Bello, A. Bikfalvi, R. S. Carroll, M. Machluf, *Clin. Cancer Res.* **2005**, *11*, 768–776.
[53] S. Duvvuri, K. G. Janoria, A. K. Mitra, *Pharm. Res.* **2006**, *23*, 215–223.
[54] M. Hakkarainen, *Adv. Polym. Sci.* **2002**, *157*, 113–138.
[55] D. Lemoine, C. Francois, F. Kedzierewicz, W. Preat, M. Hoffman, P. Maincent, *Biomaterials* **1996**, *17*, 2191–2197.
[56] S. M. Li, M. Vert, *Macromolecules* **1994**, *27*, 3107–3110.
[57] K. Makino, M. Arakawa, T. Kondo, *Chem. Pharm. Bull.* **1985**, *33*, 1195–1201.
[58] T. G. Park, *J. Controlled Release* **1994**, *30*, 161–173.
[59] T. G. Park, *Biomaterials* **1995**, *16*, 1123–1130.
[60] M. A. Tracy, K. L. Ward, L. Firouzabadian, Y. Wang, N. Dong, R. Qian, Y. Zhang, *Biomaterials* **1999**, *20*, 1057–1062.
[61] H. Tsuji, K. Ikarashi, *Polym. Degrad. Stab.* **2004**, *85*, 647–656.
[62] H. Tsuji, K. Ikarashi, *Biomacromolecules* **2004**, *5*, 1021–1028.
[63] H. Tsuji, A. Mizuno, Y. Ikada, *J. Appl. Polym. Sci.* **2000**, *77*, 1452–1464.
[64] A. Baji, S.-C. Wong, T. S. Srivatsan, G. O. Njus, G. Mathur, *Mater. Manuf. Processes* **2006**, *21*, 211–218.
[65] G. Wei, P. X. Ma, *Biomaterials* **2004**, *25*, 4749–4757.
[66] X. Qiu, Y. Han, X. Zhuang, X. Chen, Y. Li, X. Jing, *J. Nanopart. Res.* **2007**, *9*, 901–908.
[67] S.-S. Kim, M. S. Park, O. Jeon, C. Y. Choi, B.-S. Kim, *Biomaterials* **2006**, *27*, 1399–1409.
[68] H. L. Nichols, N. Zhang, J. Zhang, D. L. Shi, S. Bhaduri, X. J. Wen, *J. Biomed. Mater. Res. Part A* **2007**, *82A*, 373–382.
[69] J. D. Kretlow, A. G. Mikos, *Tissue Eng.* **2007**, *13*, 927–938.
[70] W. L. Murphy, D. J. Mooney, *J. Am. Chem. Soc.* **2002**, *124*, 1910–1917.
[71] A. Oyane, M. Uchida, C. Choong, J. Triffitt, J. Jones, A. Ito, *Biomaterials* **2005**, *26*, 2407–2413.
[72] R. Y. Zhang, P. X. Ma, *J. Biomed. Mater. Res.* **1999**, *45*, 285–293.
[73] E. Jabbarzadeh, L. S. Nair, Y. M. Khan, M. Deng, C. T. Laurencin, *J. Biomater. Sci. Polym. Ed.* **2007**, *18*, 1141–1152.
[74] A. Musyanovych, J. Schmitz-Wienke, V. Mailänder, P. Walther, K. Landfester, *Macromol. Biosci.* **2008**, *8*, 127–139.
[75] G. Reich, *Eur. J. Pharm. Biopharm.* **1998**, *45*, 165–171.
[76] A. Ethirajan, A. Musyanovych, A. Chuvilin, K. Landfester, unpublished results.
[77] N. Steiert, K. Landfester, *Macromol. Mater. Eng.* **2007**, *292*, 1111–1125.
[78] F. Tiarks, K. Landfester, M. Anonietti, *Macromol. Chem. Phys.* **2001**, *202*, 51–60.

  

[79] V. Holzapfel, A. Musyanovych, K. Landfester, M. R. Lorenz, V. Mailander, *Macromol. Chem. Phys.* **2005**, *206*, 2440–2449.
[80] K. Landfester, L. P. Ramirez, *J. Phys. Condens. Matter* **2003**, *15*, S1345-S1361.
[81] Q. Q. Hoang, F. Sicheri, A. J. Howard, D. S. C. Yang, *Nature* **2003**, *425*, 977–980.
[82] G. K. Hunter, B. L. Allen, M. D. Grynpas, P. T. Cheng, *Biochem. J.* **1985**, *228*, 463–469.
[83] J. D. Termine, H. K. Kleinman, S. W. Whitson, K. M. Conn, M. L. McGarvey, G. R. Martin, *Cell* **1981**, *26*, 99–105.
[84] A. Veis, *J. Bone Miner. Res.* **1993**, *8*, S493-S497.
[85] H. Tamai, H. Yasuda, *J. Colloid Interface Sci.* **1999**, *212*, 585–588.
[86] S. Schachschal, A. Pich, H.-J. P. Adler, *Colloid Polym. Sci.* **2007**, *285*, 1175–1180.
[87] R. Zhang, D. Zhang, H. Mao, W. Song, G. Gao, F. Liu, *J. Mater. Res.* **2006**, *21*, 349–354.
[88] D. P. Liu, P. Majewski, B. K. O'Neill, Y. Ngothai, C. B. Colby, *J. Biomed. Mater. Res. Part A* **2006**, *77A*, 763–772.
[89] A. Musyanovych, R. Rossmanith, C. Tontsch, K. Landfester, *Langmuir* **2007**, *23*, 5367–5376.
[90] A. Ethirajan, U. Ziener, K. Landfester, *Chem. Mater.* **2009**, *21*, 2218–2225.
[91] W. Liang, T. F. Tadros, P. F. Luckham, *Langmuir* **1994**, *10*, 441–446.
[92] X. E. E. Reynhout, J. Meuldijk, B. A. H. Drinkenburg, *Prog. Colloid Polym. Sci.* **2004**, *124*, 64–67.
[93] M. S. Romero-Cano, A. Martin-Rodriguez, F. J. de Las Nieves, *Langmuir* **2001**, *17*, 3505–3511.
[94] M. S. Romero-Cano, A. Martin-Rodriguez, F. J. de Las Nieves, *Colloid Polym. Sci.* **2002**, *280*, 526–532.
[95] L. Vorwerg, R. G. Gilbert, *Macromolecules* **2000**, *33*, 6693–6703.
[96] G. Busch, E. Jaehne, X. D. Cai, S. Oberoi, H. J. P. Adler, *Synth. Met.* **2003**, *137*, 871–872.
[97] A. Henke, E. Jaehne, H. J. P. Adler, *Macromol. Symp.* **2001**, *164*, 1–9.
[98] H. Park, E. Bae, J. J. Lee, J. Park, W. Choi, *J. Phys. Chem. B* **2006**, *110*, 8740–8749.
[99] J. Y. Wach, B. Malisova, S. Bonazzi, S. Tosatti, M. Textor, S. Zurcher, K. Gademann, *Chem. Eur. J.* **2008**, *14*, 10579–10584.
[100] H. Fleisch, R. G. G. Russell, M. D. Francis, *Science* **1969**, *165*, 1262–1264.
[101] R. G. G. Russell, M. J. Rogers, *Bone* **1999**, *25*, 97–106.
[102] A. Ziegler, K. Landfester, A. Musyanovych, *Colloid Polym. Sci.* **2009**, *287*, 1261–1271.
[103] A. Zeller, A. Musyanovych, M. Kappl, A. Ethirajan, D. Markova, M. Klapper, K. Landfester, **2010**, *ACS Appl. Mater. Interfaces*, in press.
[104] K. Schöller, A. Zeller, A. Ethirajan, K. Landfester, unpublished results.

Published online: July 26, 2010

  